JOURNAL OF MATERIALS SCIENCE 23 (1988) 2882–2892

Coarsening during solidification of aluminium–copper alloys

P. W. WILSON*, T. Z. KATTAMIS
Department of Metallurgy, University of Connecticut, Storrs, Connecticut 06268, USA

Y. SHIOHARA
Department of Materials Science and Engineering, Massachusetts Institute of Technology, Cambridge, Massachusetts 02139, USA

Coarsening of directionally solidified α-phase dendrites and of particulate α-phase/liquid mixtures was investigated in Al–4, 10 and 20 wt % Cu alloys, as a function of temperature, composition and presence or absence of forced convection. Isothermal dendritic coarsening in the absence of convection operated in two stages. In stage I the dendritic structure broke down through remelting into fragments which spheroidized quickly; in stage II the spherical particles coarsened slowly. The coarsening rate of the dendritic or particulate solid increased with temperature and copper dilution. Alloy inoculation with titanium slowed coarsening, yielding finer dendritic microstructures. The effect of turbulent flow on coarsening was manifested only for longer holding times. At higher impeller angular velocities the dendritic structure breaks down into fragments which spheroidize rapidly. At lower shear rates (below 650 rev min^{-1}) solid particles in solid–liquid mixtures coalesce into clusters, whereas at higher rates the clusters break up again into individual particles. A coarsening model was introduced which showed that coarsening is faster in the presence of forced convection, because of the resulting decrease in solute diffusion-boundary layer thickness.

1. Introduction

The study of dendrite coarsening kinetics is simplified if the alloy is directionally solidified under steady state conditions in the form of dendritic monocrystals or bicrystals and solidification is interrupted by quenching the remaining liquid, thus preserving the solid–liquid interface. It is then possible to measure the specific surface (surface-to-volume ratio) or perimeter (perimeter-to-area ratio) of the dendrites, S_v, and the average secondary dendrite arm spacing, $\bar{d}$, within the mushy zone at various distances from the dendrite tips, and thus at various temperatures between the liquidus and the eutectic temperature, which prevailed at the moment of quench [1, 2]. Because solidification prior to quenching takes place under steady state conditions of thermal gradient in the mushy zone, G_m, and growth velocity, R, distances divided by velocity, yield times. Thus, the evolution of dendritic morphology can be followed, and S_v or $\bar{d}$ plotted against the distance from the dendrite tips or time during which solidification had progressed.

In order to study isothermal coarsening kinetics, crystal pulling is stopped for various lengths of time prior to quenching the remaining liquid, by pneumatically thrusting the alumina tube containing the specimen into water. Thus S_v and $\bar{d}$ can be measured at various temperatures in specimens held for different lengths of time prior to quenching.

Directional solidification under steady state conditions lends itself very conveniently to the study of the effect of forced convection on coarsening kinetics, both isothermal, as well as during continuous solidification. This effect was studied for aluminium–copper alloys by generating turbulent fluid flow with a graphite impeller, and is reported in this paper.

Any liquid flow present ahead of the advancing interface may partially penetrate between the primary arms of the dendritic array but is less likely to penetrate between the narrowly spaced secondary dendrite arms because of greater resistance. Ridder *et al.* [3], investigated fluid flow during electroslag remelting and continuous casting of tin–lead alloys and evaluated macrosegregation. They concluded that natural convection in the liquid metal pool, driven by temperature or solute concentration gradients, had little effect on interdendritic fluid and resulting macrosegregation. The interaction between natural convective flow and an advancing tin–lead dendritic interface was studied by Stewart and Weinberg [4] for dendrites which grew horizontally while the liquid descend vertically along the advancing interface. Fluid flow penetration between dendrites was small.

Intuitively, it would seem that forced convection increases liquid flow penetration within the dendritic array. Such was the observation of Saski *et al.* [5] made during solidification of electromagnetically stirred carbon steel ingots. As bulk flow rate increased from 0.2 to 1.2 m sec^{-1} the fraction of solid present at

* *Present address*: Arwood Corporation, Tilton, New Hampshire, USA.

0022–2461/88 $03.00 + .12

the line of maximum penetration rose from 30% to 70%, hence penetration itself increased. Momono and Ikawa [6], studied the interdendritic fluid flow penetration in Al–3 wt % Cu alloy at flow rates reaching 12 cm sec^{-1} and the effect of electromagnetic stirring on the mixing of interdendritic solute-rich liquid with the bulk liquid.

The penetration of fluid moving slowly in an upward advancing dendritic array in aluminium alloys with silicon, copper or magnesium was investigated by Gabathuler and Weinberg [7] who produced controlled fluid flow by a flat rotating disc immersed in the liquid. Bulk liquid penetration was determined by a radioactive tracer added to the melt. The downward flow penetration into the interdendritic spaces was found to depend on disc angular velocity, distance between disc and dendrite tips, temperature gradient and hence dendrite length in the mushy zone and interdendritic liquid density gradient. Disc velocity was the most important factor and penetration increased with it.

The accelerating effect of forced convection on dendritic coarsening was previously indicated [8–10]. This effect was quantitatively evaluated in the present investigation. During coarsening of directionally grown dendrites in the presence of forced convection it was observed that at high impeller velocities dendritic structure degenerated into a particulate structure consisting of particles surrounded by liquid. Thus, it was decided that the effect of convection should also be studied on the coarsening of particulate α-phase/liquid mixtures in aluminium–copper alloys. One of the directions of the present study was the effect of composition on coarsening kinetics. The relative amounts of solid and liquid present depend on temperature and affect interdendritic liquid composition. They are, therefore, important in establishing coarsening kinetics [11]. As it is not possible over a range of compositions to hold both temperature and fraction solid constant, the experiments were conducted at constant fraction solid.

Spencer *et al.* [12] studied the rheology of semi-solid Sn–15 wt % Pb alloy. They found that when the alloy was cooled from above the liquidus to the desired final fraction solid while continuously sheared, the shear stress required for flow was reduced by about three orders of magnitude and the mixture behaved like a thixotropic particulate solid–liquid slurry, whose apparent viscosity increased with fraction solid and decreased as particles became more spherical.

2. Experimental procedure

2.1. Coarsening of directionally solidified dendrites

The alloy specimens were placed in alumina or mullite tubes (0.006 m i.d. × 0.5 m long) and directionally solidified under an average thermal gradient in the mushy zone of 4.5×10^3 K m^{-1} at a growth rate of 0.30 m h^{-1}, as previously described [2]. In a first series of experiments the dendritic growth was interrupted by quenching the remaining liquid. A thermocouple inserted along the specimen axis indicated variation of temperature with location or time. The liquidi of Al–Cu alloys used here are fairly accurately known. Thus, the temperature at a given location at the moment of quench could be determined. This series of runs was used to study the combined effects of coarsening and growth during continuous solidification. In each specimen various transverse sections were made perpendicular to the growth direction at temperatures between the equilibrium liquidus and the eutectic temperature, 821.2 K. In each section, S_v was determined by quantitative metallography [13] and plotted against time during which solidification progressed. Secondary dendrite arm spacings were measured in longitudinal sections at the same temperature levels.

In a second series of experiments the withdrawal of the furnace plus chill assembly was stopped for various lengths of time, up to 900 sec, prior to quenching. The temperature at various locations within the mushy zone at the time of quench was determined using two thermocouples which were inserted axially from the top of the crucible and whose tips were 0.001 m apart. When furnace withdrawal was stopped the steady state motion of the solid–liquid interface ceased and the heat flow conditions, and hence the temperature distribution in the mushy zone, were modified. Transverse sections were made in the specimens at various temperatures between the liquidus and the eutectic and S_v determined with variation in temperature and holding time. Some runs were made in larger cylindrical graphite moulds (2.8×10^{-2} m i.d. × 0.254 m long). Crucible pulling was interrupted and the advancing dendritic array stopped and coarsened for up to 480 sec prior to quenching. In some runs a graphite impeller (0.25 m diameter × 0.37 m high) was introduced in the melt at about 0.1 m from the dendrite tip plane, as soon as crucible pulling was stopped. It was removed prior to quenching. Most of the runs were carried out at 42 rev. min^{-1} at which fluid flow was turbulent.

2.2. Coarsening of particulate solid–liquid mixtures

The alloys were cast in moulds (0.083 m diameter × 0.15 m long) made of "fiberchrome", an insulating material, backed by sand and placed on water-cooled copper chill plates. The alloys were prepared by melting in a clay–graphite crucible the proper amounts of aluminium (99.995%) and an Al–48.6 wt % Cu master alloy. Cylindrical castings of each alloy were made in these moulds. An additional ingot of inoculated alloy was made by adding 0.1 wt % Ti, in the form of an aluminium–titanium master alloy, to molten Al–4 wt % Cu.

Each of these ingots was sectioned longitudinally and the dendritic structure revealed. S_v was measured at various locations, using lineal analysis [13]. Disc-shaped slabs, 0.005 m thick were cut from each ingot at locations at which the secondary dendrite arm spacings were the same. Within each disc the spacing was quite uniform due to the presence of insulating "fiberchrome" and the resulting low lateral thermal gradients.

Approximate temperatures were selected from each

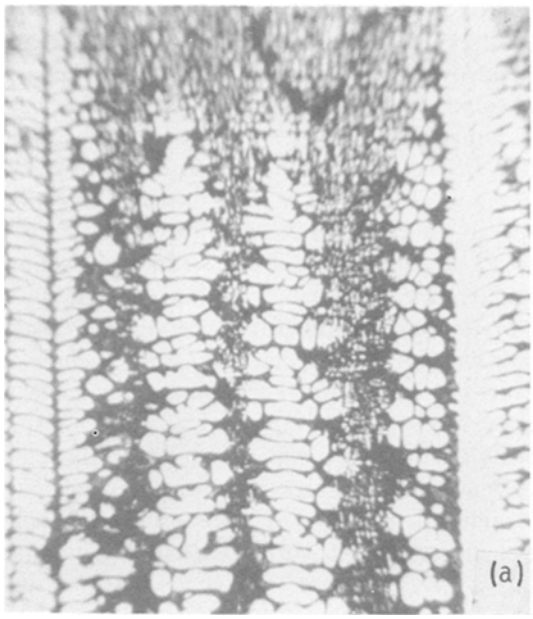

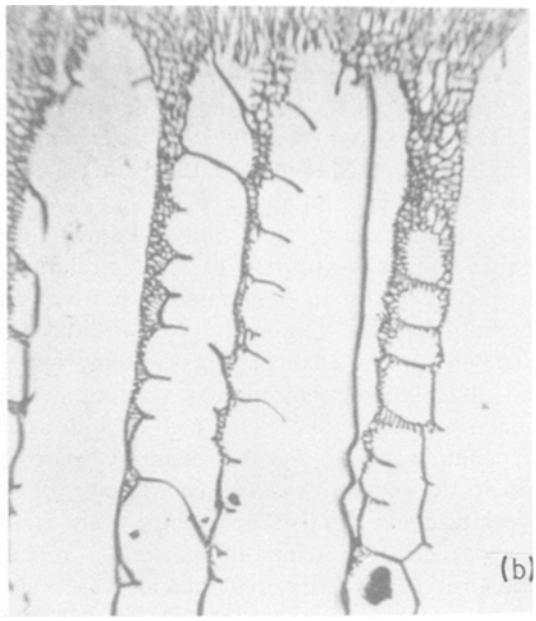

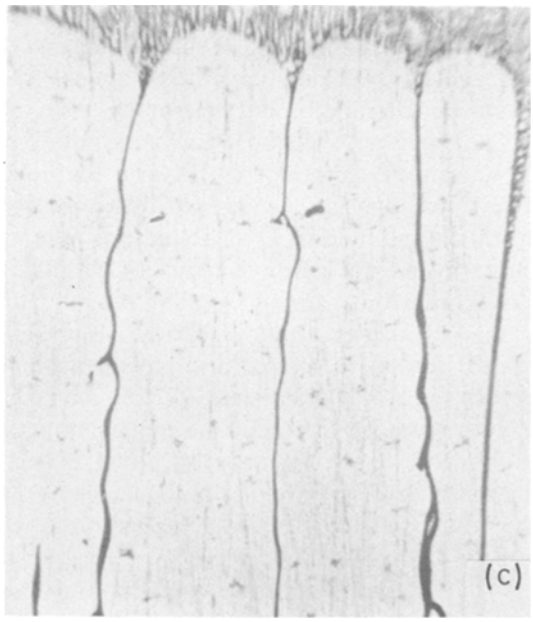

Figure 1 Photomicrographs of longitudinal sections of directionally solidified and interface-quenched Al–4 wt % Cu dendritic monocrystals pulled at 0.30 m h^{-1}, × 100. Holding times prior to quenching were: (a) 0, (b) 150 and (c) 900 sec.

alloy corresponding to fractions solid of 0.3, 0.4 and 0.5, as predicted by the Scheil equation modified by Brody and Flemings [14]. The samples were placed in alumina crucibles packed with alumina powder for support at temperatures at which a high volume fraction liquid is present. A thermocouple was inserted in the specimens for temperature measurement. The specimens were isothermally held for 1, 7, 24 and 48 h and were subsequently water-quenched. They were sectioned, polished and etched. For each specimen the solid–liquid specific interfacial area, S_v, and average particle radius, $\bar{r}$, were determined with lineal analysis [13].

In order to study the effect of forced convection on coarsening kinetics of particulate solid–liquid mixtures, melts of Al–4 wt % Cu and Al–20 wt % Cu were superheated by about 50 K above the liquidus. Stirring was then initiated with a graphite propeller (0.0254 m diameter) at 130 rev. min^{-1}, while the temperature was slowly lowered to that corresponding in each case to a fraction solid $f_s = 0.4$. At that temperature, stirring velocities were varied and the specimens held isothermally for up to 10 h prior to quenching the remaining liquid.

3. Results and discussion

3.1. Coarsening of columnar dendrites

Photomicrographs of longitudinal sections of Al–4 wt % Cu alloy specimens which were pulled at 0.30 m h^{-1} and quenched after holding for various times, are illustrated in Fig. 1. The variation of dimensionless specific surface, S_v/S_{vo}, with isothermal holding time is illustrated in Fig. 2 for this alloy at 833, 863 and 916 K corresponding to volume fractions solid of 0.91, 0.86 and 0.24, respectively. For each temperatures, S_{vo} was measured in a dendritic specimen which was pulled and quenched without holding. Coarsening is faster at higher temperatures, and hence at lower volume fractions of solid. Fig. 3 allows a comparison of isothermal coarsening kinetics of Al–4, 10 and 20 wt % Cu at 863 K. Coarsening is faster for more dilute alloys, as also confirmed by Fig. 4 which illustrates the variation of dimensionless secondary dendrite arm spacing, $\bar{d}/\bar{d}_0$, with holding time for the same alloys and temperature.

The increase in $\bar{d}/\bar{d}_0$ with duration of solidification or temperature difference from the liquidus is shown in Fig. 5 for Al–4, 10 and 20 wt % Cu alloys which were cooled at 0.37 K sec^{-1}. In each case $\bar{d}_0$ is the average secondary dendrite arm spacing very close to the dendrite tips. The terminal point on each curve corresponds to completion of solidification. Again, at a given moment dendrites are coarser for more dilute alloys.

The effect of turbulent convection on the coarsening behaviour of directionally grown Al–20 wt % Cu dendrites is illustrated in Fig. 6. The specimen of Fig. 6a was quenched immediately after pulling was stopped.

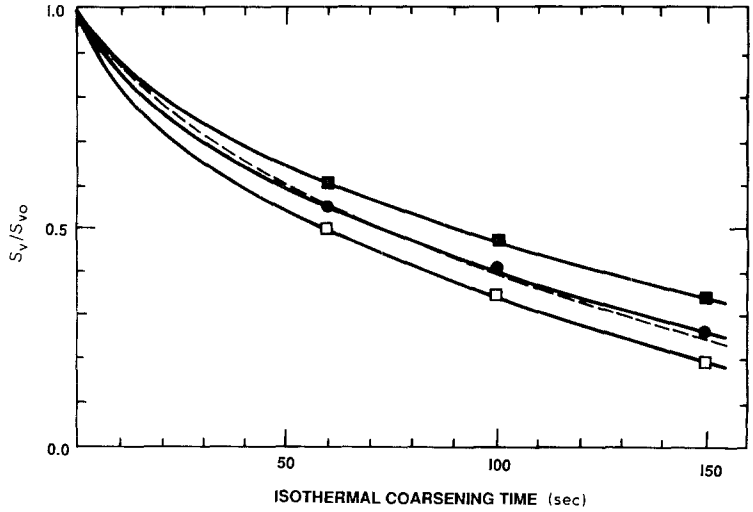

Figure 2 S_v/S_{vo} against isothermal coarsening time at three different temperatures, for Al–20 wt % Cu alloy. (■) 833 K, $f_s = 0.91$, $S_{vo} = 0.8 \times 10^5 m^{-1}$, (●) 863 K, $f_s = 0.86$, $S_{vo} = 1.3 \times 10^5 m^{-1}$; (□) 916 K, $f_s = 0.24$, $S_{vo} = 2.6 \times 10^5 m^{-1}$. (——) Experimental, (– – –) theoretical curves.

The specimens of Figs 6b and c were held stationary for 480 sec prior to quenching. During this holding the dendritic solid coarsened in the absence of stirring, Fig. 6b, or in the presence of stirring at 42 min^{-1}, Fig. 6c. The effect of stirring on coarsening is noticeable. Forced convection affects the dendritic microstructure by accelerating coarsening and by modifying the temperature gradient distribution in the mushy zone.

The variation of $\bar{d}/\bar{d}_0$ and S_v/S_{vo} with isothermal holding time at 863 K is shown in Figs 7 and 8 in the presence or absence of stirring. The initial quantities $\bar{d}_0$ and S_{vo} were measured at 863 K in the specimen which was continuously pulled and quenched without any holding or forced convection. Again the effect of stirring on coarsening is detectable but not significant. It may be assumed that the fluid flow generated by the graphite impeller did not penetrate appreciably into the interdendritic regions, because: (1) they are narrow and only waves shorter than their width can penetrate therein; (2) in aluminium–copper alloys, the interdendritic liquid is richer in copper, and hence heavier than the bulk liquid ahead of the primary dendrite tips. Maximum liquid density is at the eutectic isotherm. The density gradient constitutes a barrier opposing penetration at low flow velocities.

It is not possible to calculate the distribution of turbulent flow velocities generated by an impeller of complex geometry as a function of location and time. In a model introduced by Levich [15, 16] the turbulent flow is considered to consist of a series of random, unsteady perturbations of the local instantaneous fluid velocity. These perturbations, or eddies, are periodic with incommensurable frequency and are superimposed on the same flow. A velocity, V, and a length, l, over which the velocity is roughly constant for a particular region of fluid [15] are associated with turbulent flow. When the viscous force of the fluid equals the inertial force, the corresponding eddy length, l_0, and velocity V_0, are given by [15]

$$l_0 = r/(Re_R)^{3/4} \quad \text{and} \quad V_0 = v/l_0 \qquad (1)$$

where r is the stirrer radius ($r = 0.0127$ m), $Re_R = \omega r^2/\nu_m$ is the stirrer Reynolds number, ω is angular velocity of the stirrer ($\omega = 2\pi N$ rad sec^{-1} and N is rev. sec^{-1}), ν_m is kinematic viscosity of the liquid. The eddy length, l_0, is also known as the "microscale of turbulence". In the present case, at least at the early stages of stirring there are no solid particles in suspension in the liquid, hence $\nu_m \cong \nu \cong 10^{-6} m^2 sec^{-1}$. From these data $l_0 = 54.3 \times 10^{-6}$ m. Penetration in the spaces of the order of l_0 would then be possible. However, the spaces between secondary dendrite arms are much smaller than 54.3 μm and flow penetration in these is not expected to be significant. Thus, the effect of turbulent convection at 42 rev. min^{-1} is not expected to be important.

A run was then conducted using a stainless steel

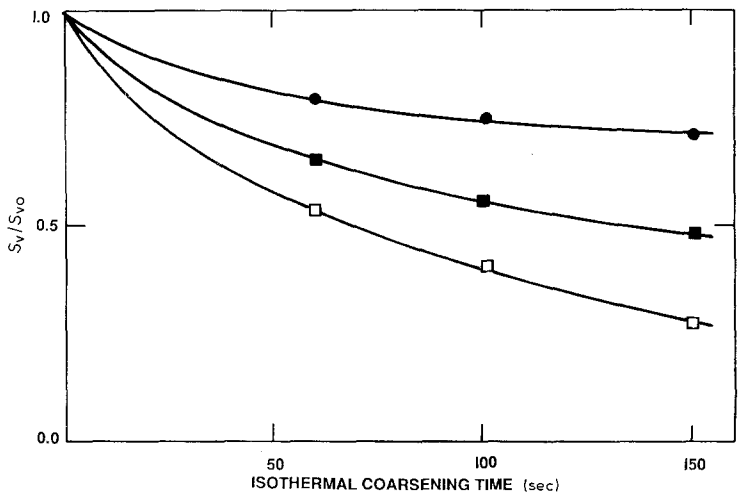

Figure 3 S_v/S_{vo} against isothermal coarsening time at 863 K. (□) Al–4, (■) 10 and (●) 20 wt % Cu alloys, for $f_s = 0.86$, 0.58 and 0.05, and $S_{vo} = 4.0 \times 10^5$, 4.8×10^5 and $6.4 \times 10^5 m^{-1}$ respectively.

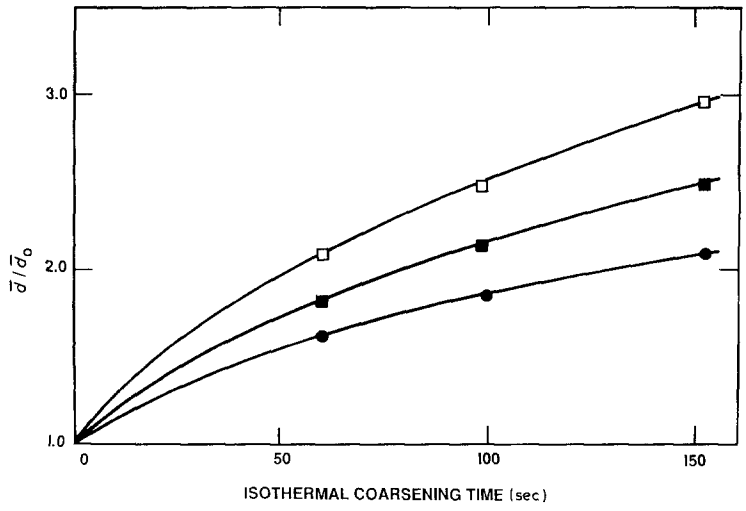

Figure 4 $\bar{d}/\bar{d}_0$ against isothermal coarsening time at 863 K. (□) Al–4, (■) 10 and (●) 20 wt % Cu alloys, for f_s = 0.86, 0.58, 0.05 and $\bar{d}_0$ = 18, 14 and 10 μm, respectively.

impeller coated with zirconium silicate wash at 950 rev. min^{-1}. This impeller had the same diameter as the graphite impeller used above at 42 rev. min^{-1}, but had a different blade geometry. At this velocity the microscale of turbulence was reduced to 5.23 μm and turbulent flow apparently penetrated the spaces between secondary dendrite arms causing remelting at their roots and detachment. Fig. 9 shows that the uniformity of the dendritic array has been completely destroyed and that clusters of dendrite arm debris with local eutectic regions have formed, yielding a typical duplex ("rheocast") structure.

3.2. Coarsening of particulate solid–liquid mixtures

The initial microstructures chosen for the various specimens exhibited an average $S_{v_0} = 2 \times 10^4 m^{-1}$ and an average dendrite arm radius $\bar{r}_0 = 12 \mu m$. Fig. 10 illustrates the isothermal evolution of microstructure of Al–4 wt % Cu alloy specimens at 908 K, for up to 24 h. Through coarsening of the solid (or the initial liquid inclusions) the dendritic network is destroyed, and detached dendrite arms or debris spheroidize and coarsen, Figs 10b and c. Some of the particles coalesce. The initial rapid decrease in S_v/S_{v_0}, Fig. 11, corresponds to the breaking up of the dendrites and the formation of small spheres. Subsequent coarsening of the spheres is substantially slower. This figure illustrates the effect of fraction solid or temperature on isothermal coarsening kinetics. Fig. 12 confirms that at a given volume fraction solid and for a given isothermal coarsening time, the coarsening rate of particulate solid increases with decreasing solute concentration in the alloy. The same figure illustrates the isothermal coarsening behaviour of Al–4 wt % Cu–0.1 wt % Ti, an alloy which is grain-refined by titanium. The presence of titanium slows coarsening.

Fig. 13 illustrates the microstructures of two Al–20 wt % Cu alloy specimens which were cooled from the superheated state while being stirred at 22 and 130 rev. min^{-1}, respectively. These specimens were quenched as soon as the temperature reached 829 K, at which f_s = 0.4. At lower stirrer angular velocities equiaxed dendrite rosettes predominate, whereas at higher velocities spheroidized particles, either isolated or coalesced, are observed. During the later stages of the cooling period, as well as during the isothermal holding period at low shear rates, the solid particles coalesce into clusters, Fig. 14. At shear rates above 650 rev. min^{-1} the aggregates appear to break up back into individual particles. Similar observations were made by Michaels and Bolger [17], in flocculated aqueous kaolin suspensions. At low shear rates the flocs grouped into aggregates which sometimes formed networks extending to the walls of the containers and gave the suspension a finite yield strength. At high shear rates the aggregates broke up into individual flocs.

The effect of stirring at 130 rev. min^{-1} on isothermal coarsening at 829 K is shown in Fig. 15, where S_v/S_{v_0}

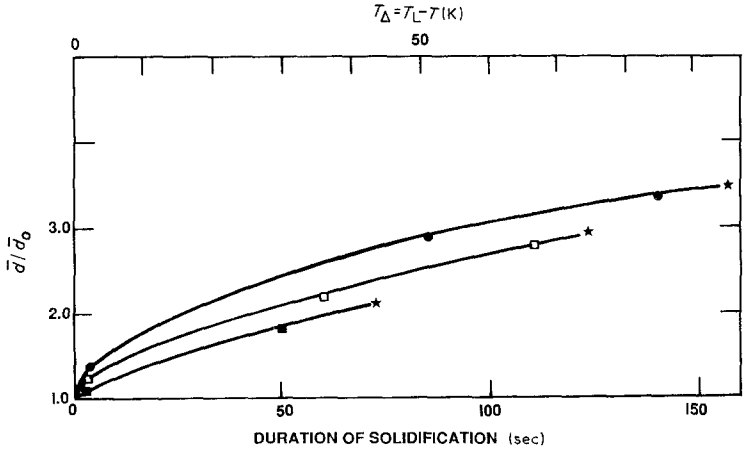

Figure 5 Variation of $\bar{d}/\bar{d}_0$ with duration of solidification or temperature difference from the liquidus. Experimental curves for (●) Al–4, (□) 10 and (■) 20 wt % Cu alloys cooled at about 0.37 K sec^{-1}, for $\bar{d}_0$ = 25, 20 and 14 μm, respectively.

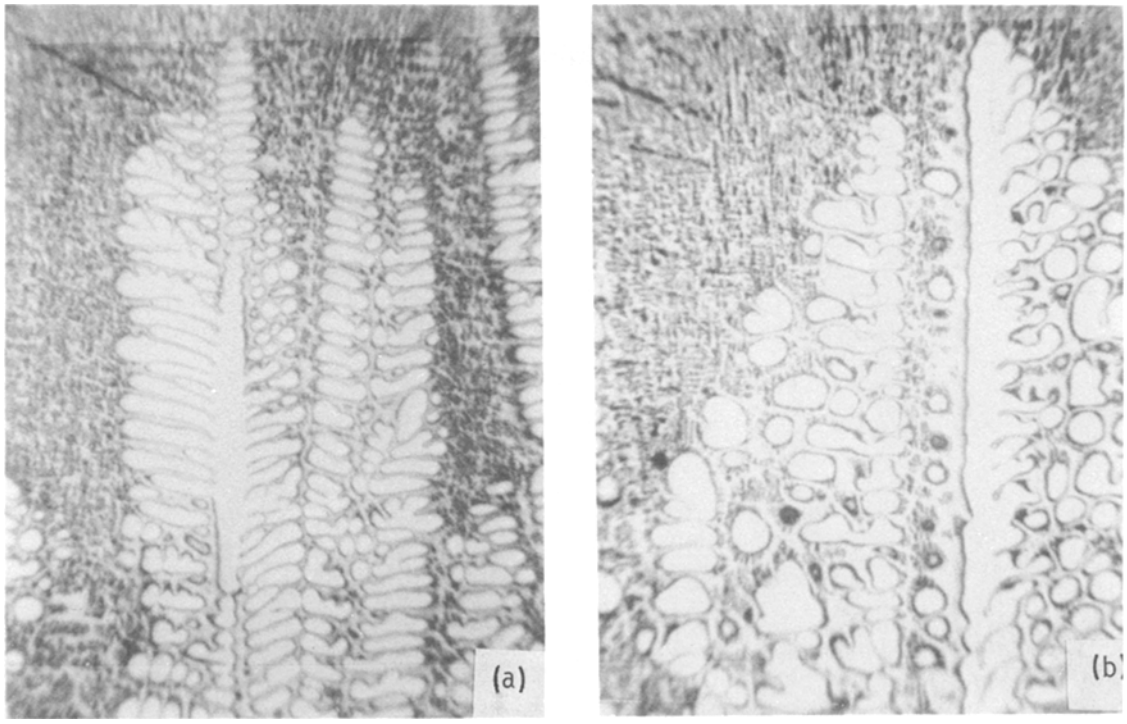

Figure 6 Photomicrographs of Al–20 wt % Cu alloy specimens directionally solidified, × 50. Pulling was stopped for 480 sec prior to quenching the remaining liquid: (a) no stirring, (b) stirring at 42 rev. min^{-1}.

was plotted against isothermal coarsening time and compared with a plot for specimens that were not stirred. The acceleration of coarsening due to stirring, which becomes more important for longer times, is well established. A similar conclusion can be formulated by examining Fig. 16, in which the dimensionless average particle size $\bar{r}/\bar{r}_0$ is plotted against isothermal coarsening time for specimens which were held at 829 K, without or with stirring at 130 rev. min^{-1}. The effect of stirring speed on isothermal coarsening kinetics at a given temperature is shown in Fig. 17, where S_v/S_{vo} is plotted against stirring speed for Al–20 wt % Cu specimens that were held at 829 K for 10 h.

During isothermal coarsening, the initial dendritic structure partially remelted and underwent dramatic changes, Fig. 10. Intradendritic liquid inclusions coarsened rapidly, generating dendritic fragments which spheroidized very fast. This first stage of rapid coarsening corresponds to the sharp decrease in S_v/S_{vo} for short times, Figs 11 and 12. From then on, coarsening of the spheres, which constitutes the second stage, is rather slow because: (1) particle radii are already large; and (2) spherical particle size is relatively uniform, hence the driving force for coarsening is greatly reduced.

3.3. Modelling of coarsening

The breaking up of the dendrites into fragments which quickly spheroidize is morphologically a very intricate process and its mathematical description is very complex. On the other hand, coarsening of dispersed spheres in the liquid during the second stage of the process can be treated as previously done [18].

Applying that analysis to a system of n spherical particles of radii $r_1, r_2, \ldots, r_i, \ldots, r_j, \ldots, r_n$, and

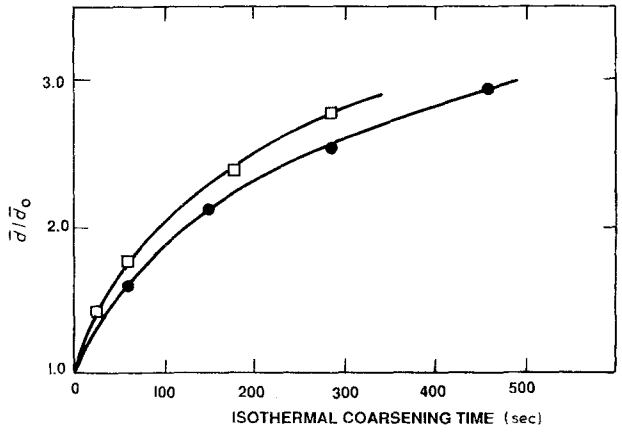

Figure 7 $\bar{d}/\bar{d}_0$ against isothermal holding time at 863 K. Al–20 wt % Cu alloy, f_s = 0.05. Comparison between (●) unstirred melt and (□) melt stirred at 130 rev. min^{-1}.

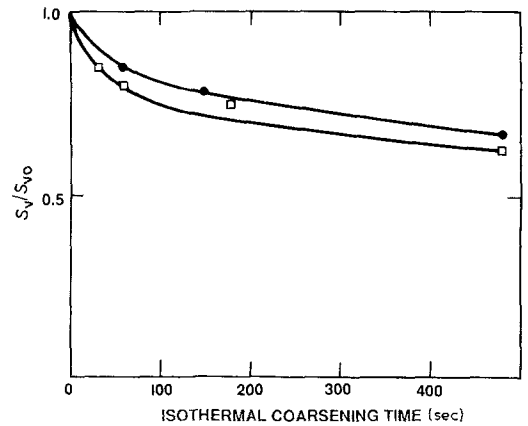

Figure 8 S_v/S_{vo} against isothermal coarsening time at 863 K. (●) Unstirred melt and (□) melt stirred at 130 rev. min^{-1} Al–20 wt % Cu alloy, f_s = 0.05.

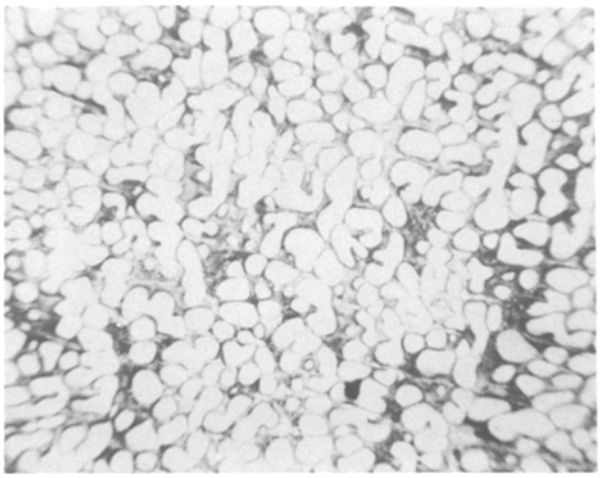

Figure 9 Photomicrograph of an Al–20 wt % Cu alloy specimen directionally grown. Pulling was stopped and stirring at 950 rev. min^{-1} was applied for 60 sec prior to quenching, × 44.

assuming that the total volume of solid remains constant during isothermal holding, which implies that back-diffusion in the solid and isothermal solidification can be neglected, it can be shown that [18]

$$\frac{dr_i}{dt} = \sum_{\substack{j=1 \\ j\neq i}}^{n} \left\{ \frac{-D\sigma T}{C_L(1-K)m_L H r_i} \left[\frac{1}{r_i} - \frac{1}{r_j}\right] \times \mathcal{H}(r_j - r_i) + \frac{-D\sigma T r_j}{C_L(1-K)m_L H r_i^2} \left[\frac{1}{r_i} - \frac{1}{r_j}\right] \times \mathcal{H}(r_j - r_i) \right\} \quad (1)$$

where $\mathcal{H}(\alpha - \beta) = 0$, for $\alpha < \beta$; $\mathcal{H}(\alpha - \beta) = 1$, for $\alpha > \beta$, and $\mathcal{H}$ is the Heaviside function, and r_i, r_j, are the radii of any two particles i and j, T is absolute temperature, C_L is solute concentration in the liquid at the interface (wt %), K is the equilibrium partition ratio, D is the solute diffusivity in the liquid ($m^2 sec^{-1}$), m_L is the liquidus slope (K/wt %), σ is the solid–liquid interfacial tension ($J^2 m^{-2}$) and H is the volumetric heat of fusion ($J m^{-3}$).

The radius of particle i as a function of time is then given by

$$r_i = r_o + \int_o^t \left(\frac{dr_i}{dt}\right) dt \quad (2)$$

and the surface-to-volume ratio by

$$S_v = \frac{\sum_i^n 4\pi r_i^2}{\sum_{i=1}^n \frac{4}{3}\pi r_i^3} \quad (3)$$

Thus, the radii of all the particles in the system can be calculated at any time from Equations 1 and 2 and S_v from Equation 3. At a given time, t, after initiation of the second stage of coarsening

$$S_v = S_{vo} + \Delta S_v \quad (4)$$

where S_{vo} refers to the particle population at the beginning of the second-stage coarsening.

This analysis was applied to Al–4 wt %Cu alloy. The following numerical values were assigned to various parameters of Equation 1: $m_L = 3.3$ K wt %, $K = 0.17$, $\sigma = 5.02 \times 10^{-2} J m^{-2}$, $H = -1.15 \times 10^9 J m^{-3}$, $D = 5 \times 10^{-14} m^2 sec^{-1}$ [19], $T = 909$ K ($f_s = 0.5$) and $C_L = 7.10$ wt % Cu. An initial population of 18 spheres was assumed, whose radii were selected randomly from specimens which were coarsened for 75 min and quenched. This time corresponds approximately to the end of the first stage of coarsening, Fig. 11. The radius of each spherical particle and the S_v for each specimen were then calculated. S_{vo} of the initial sphere population was $5 \times 10^3 m^{-1}$. In Fig. 11 the theoretical and experimental curves are

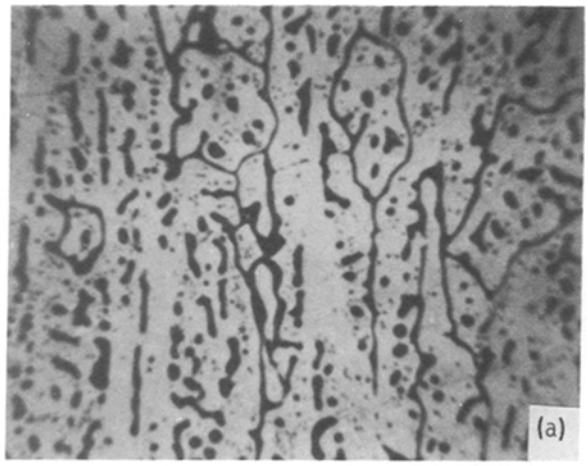

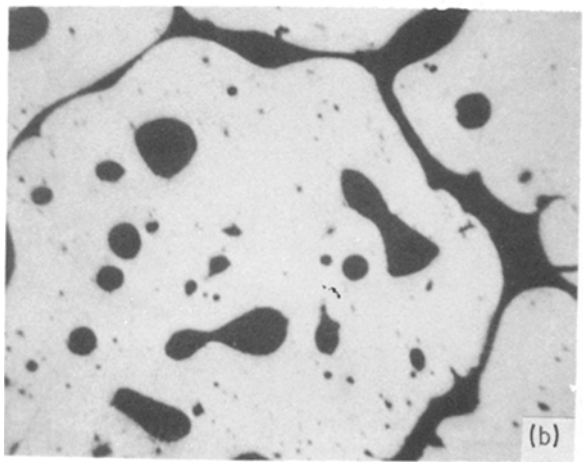

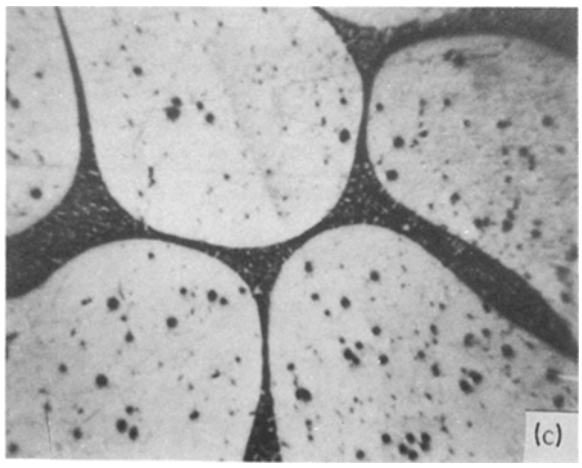

Figure 10 Photomicrographs of Al–4 wt % Cu alloy specimens isothermally held at a fraction solid $f_s = 0.5$ ($T = 908$ K) for (a) 0, (b) 1 and (c) 24 h, × 88.

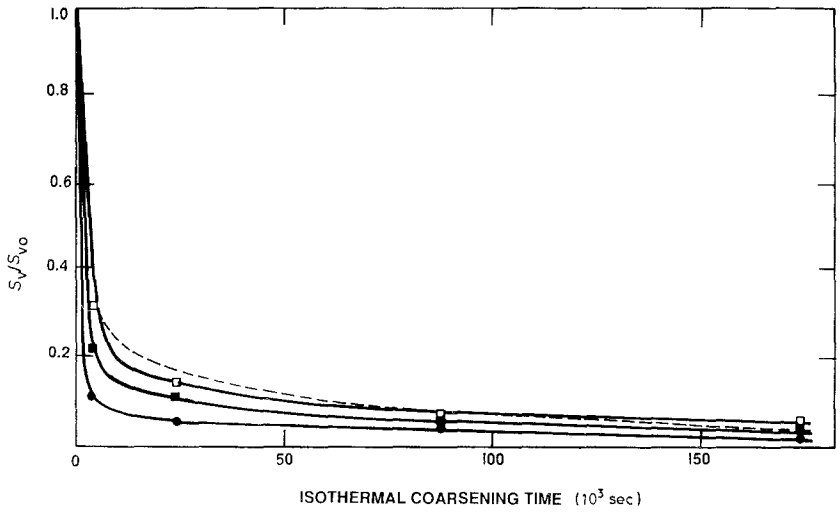

Figure 11 S_v/S_{vo} against isothermal coarsening time for different volume fractions solid or temperatures. Experimental and analytical curves for Al–4 wt % Cu alloy specimens. Experimental curves: (●) $f_s = 0.3$, $T = 915$ K, (■) $f_s = 0.4$, $T = 912$ K, (□) $f_s = 0.5$, $T = 909$ K. Analytical curve (– – –) $f_s = 0.5$, $T = 909$ K.

compared. The agreement between them is satisfactory in view of the geometric approximations of the model and the uncertainties of values assigned to various parameters.

Fig. 11 reaffirms that the coarsening rate for a given alloy increases with decreasing fraction solid of increasing temperature. T is in agreement with Equation 1 which shows that coarsening rate is proportional to temperature, but also depends on temperature implicity in a complex way, because σ, D, H and C_L are all functions of temperature. Fig. 12 shows that for a given fraction solid the coarsening rate increases with decreasing copper concentration. It is clear that the temperatures at which Al–4% Cu and Al–20% Cu alloys exhibit the same fraction solid are different, 909 and 829 K, respectively. Equation 1 roughly indicates that coarsening rate is inversely proportional to initial copper concentration, although σ, D and H also depend on composition in addition to temperature. Fig. 12 depicts the decrease in coarsening rate of Al–4 wt % Cu alloy when it is inoculated with 0.1 wt % Ti. This inoculation refines the cast grain and apparently tends to refine the dendritic structure too. The effect of titanium on slowing coarsening is negligible during solidification at the usual rates. However, it is noticeable during isothermal coarsening for a long period of time, especially at higher temperatures. If titanium is assumed to be surface active, it is possible that it reduces the dendrite–liquid interfacial tension and hence slows coarsening. However, this is an oversimplification.

To understand the effect of stirring on coarsening it is necessary to examine the magnitude of the "microscale of turbulence", l_o, or eddy length as a function of rotation rate, Equation 1. As an example, at $f_s = 0.4$, the density of the slurry, ϱ_m is related to those of the solid, ϱ_s and the liquid, ϱ_L, by: $1/\varrho_m = (0.4/\varrho_s) + (0.6/\varrho_L)$. For the solid, $\varrho_s = 2.76\,g\,cm^{-3}$ was calculated by considering the average copper concentration within the solid particles and the densities of aluminium and copper. $\varrho_L = 2.38\,cm^{-3}$ was calculated in the same way. It was found that $\varrho_m = 2.55\,g\,cm^{-3}$. For want of any better information, the viscosity was assumed to be equal to that of an Sn–15 wt % Pb slurry at $f_s = 0.4$, namely $\eta_m = 5$ P [12]. Thus, the kinematic viscosity is $5/2.55 = 1.96\,cm^2\,sec^{-1}$. For $N = 130$ rev. min^{-1}, $Re_R = 84.6$ and $l_o = 0.0455$ cm. At these very low Re_R values there is no turbulence. However, the real situation is more complicated than this. The kinematic viscosity depends not only on volume fraction solid, but also on the shape and size of solid particles and on shear rate [12]. Also, at a given shear rate or stirring velocity, because the average particle size and particle number density (number of particles per unit volume of slurry) change with time, the kinematic viscosity would be expected

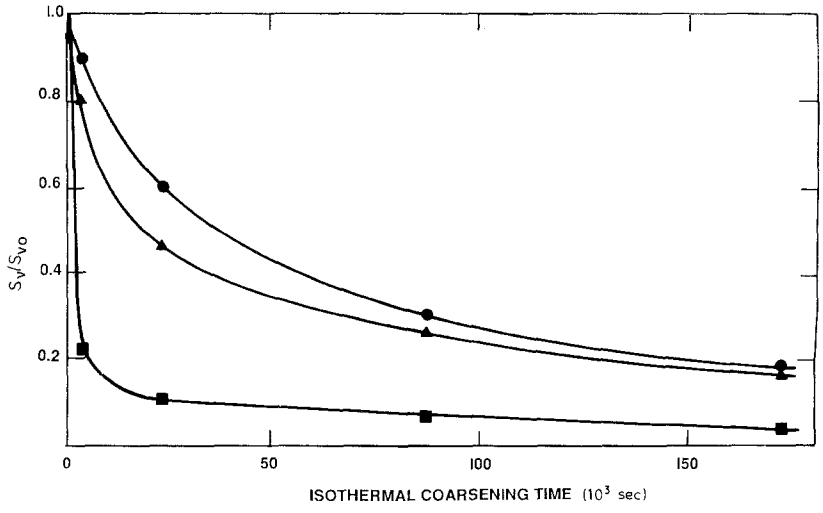

Figure 12 S_v/S_{vo} against isothermal coarsening time for $f_s = 0.4$. (■) Al–4 wt % Cu, $T = 912$ K, $S_{vo} = 5.1 \times 10^4\,m^{-1}$; (●) Al–20 wt % Cu, $T = 829$ K, $S_{vo} = 9.4 \times 10^4\,m^{-1}$, (▲) Al–4 wt % Cu–0.1 wt % Ti, $T = 912$ K, $S_{vo} = 5.1 \times 10^4\,m^{-1}$.

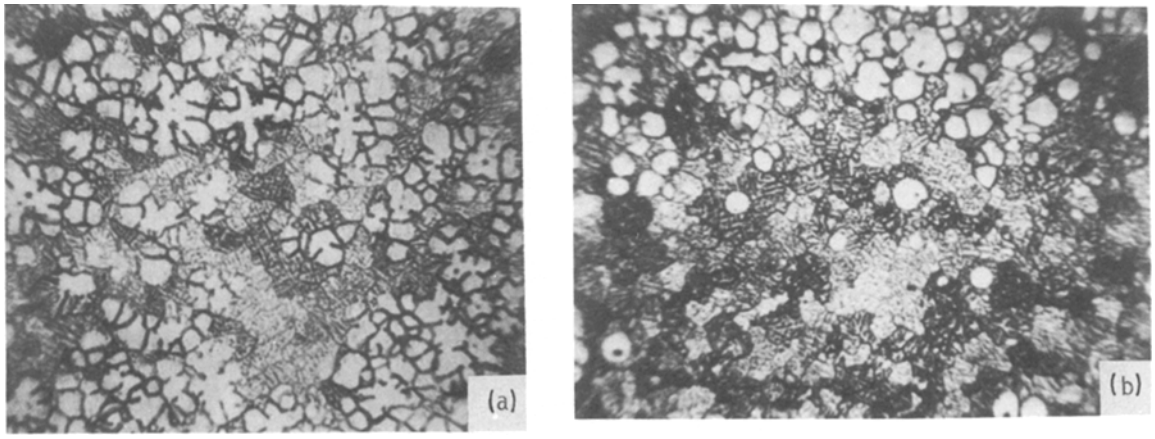

Figure 13 Photomicrographs of Al–20 wt % Cu alloy specimens which were cooled from the superheated melt state while being stirred at: (a) 22 and (b) 130 rev. min^{-1}. The specimens were quenched at 829 K (f_s = 0.4), × 44.

to change too. It can be assumed that very roughly this viscosity is an order of magnitude smaller than 1.96 $cm^2 sec^{-1}$, hence, Re_R = 110 for N = 130 rev. min^{-1} and 840 for N = 1000 rev. min^{-1}. The corresponding values of l_o would then be 373 and 81 μm, respectively. Finally, it should be remembered that the particle distribution within the slurry is not uniform and it is possible that momentarily there are no particles at all in the vicinity of the impeller, hence the kinematic viscosity will drop to that of the melt, or about 10^{-2} $cm^2 sec^{-1}$. Then, at N = 130 rev. min^{-1}, Re_R = 2171 and l_o = 39 μm, whereas at N = 1000 rev. min^{-1}, Re_R = 16 700 and l_o = 8.6 μm. These numbers correspond to complete turbulence in the vicinity of the impeller, whose pumping effect would then be substantial.

The accelerated coarsening of the solid by stirring may be explained by the resulting reduction in solute diffusion boundary layer thickness around growing or dissolving particles. Solute transport by diffusion occurs only across these thin boundary layers, whereas across the remaining distances between particles it occurs much faster by convection than by pure diffusion.

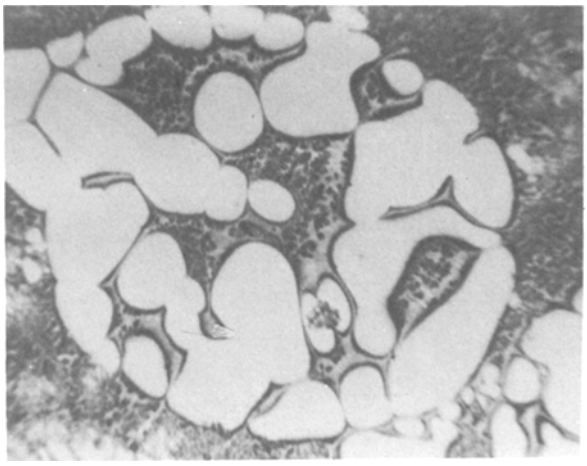

Figure 14 Photomicrograph of Al–2 wt % Cu alloy specimen which was cooled from the superheated melt state in presence of stirring at 130 rev. min^{-1} and held at 829 K (f_s = 0.4) for 1 h while stirring continued at the same velocity, × 44.

The previous isothermal coarsening analysis was applied to Al–20 wt % Cu alloy at 829 K (f_s = 0.4), using an initial population of 18 spheres (r_1 = 30, r_2 = 40, r_3 = 45, r_4 = 60, r_5 = 65, $r_{6,7,8}$ = 70, r_9 = 80, r_{10} = 90, r_{11} = 100, r_{12} = 100, r_{13} = 100, r_{14} = 115, r_{15} = 120, r_{16} = 150, r_{17} = 160, r_{18} = 160 μm) and the same values for m_L, σ, H and D. In this case, T = 829 K and C_L = 30.1 wt % Cu. The resulting analytical curve is shown in Fig. 1. Using the same particle population and parameter values and replacing D by a global mass transport coefficient, M, several curves were calculated and the plotted for various values of M. The analytical curve which was closest to the experimental curve for coarsening in the presence of stirring, Fig. 1, was found to correspond to M = 1.4D. It was then concluded that the contribution of convection to the global mass transport coefficient was 0.4D.

The main contribution of convection is to reduce the thickness of the solute diffusion boundary layer, δ, surrounding each particle. Assume first a system consisting of two spheres of α-phase surrounded by melt at temperature, T. Let a be the radius of the smaller, shrinking sphere and R that of the larger, growing sphere. The solute balance for the dissolving particle may be written as [18]

$$C_L^a(1 - K)\varrho^4\pi a^2 \frac{da}{dt} = -D\varrho r\pi a^2 \frac{C_L^a - C_L^\infty}{\delta} \quad (5)$$

where C_L^a is the concentration of solute in the liquid at T in equilibrium with a surface of radius a, C_L^∞ is the concentration in the liquid beyond the diffusion boundary layer, ϱ is density, δ is the thickness of the diffusion-boundary layer and D is solute diffusivity in the liquid. From Equation 5 it follows that

$$\frac{da}{dt} = \frac{D(C_L^\infty - C_L^a)}{\delta C_L^a(1 - K)} \quad (6)$$

Assuming that [17]

$$C_L^\infty - C_L^a \cong C_L^R - C_L \quad (7)$$

letting $C_L^a = C_L$ and remembering that [11]

$$C_L^R - C_L^a = \frac{\sigma T}{mH}\left(\frac{1}{R} - \frac{1}{a}\right) \quad (8)$$

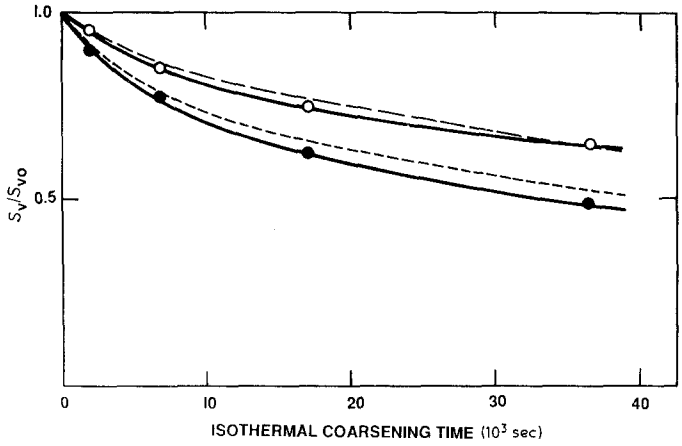

Figure 15 S_v/S_{vo} against isothermal coarsening time for specimens that were held isothermally at 829 K (●) with stirring at 130 rev. min^{-1}, or (○) without stirring. Al–20 wt % Cu alloy. Experimental, and (– – –), (– – – –) analytical curves, without and with stirring, respectively. (——) $S_{vo} = 9.4 \times 10^4 m^{-1}$, $\delta = 55 \mu m$.

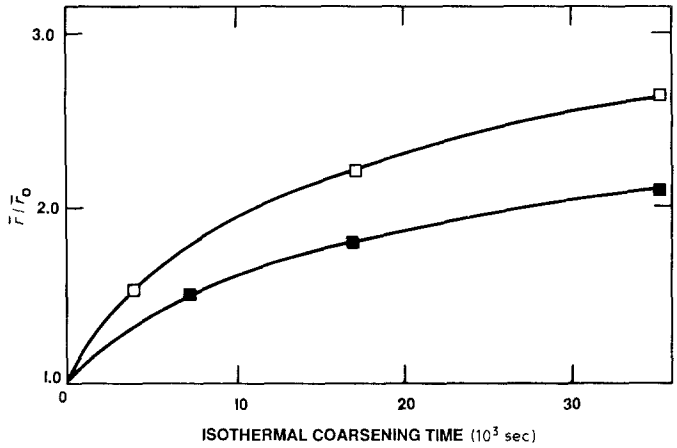

Figure 16 $\bar{r}/\bar{r}_0$ against isothermal coarsening time at 829 K ($f_s = 0.4$), (■) without or (□) with stirring at 130 rev. min^{-1}. Al–20 wt % Cu alloy, $\tau_0 = 75 \mu m$.

Equation 6 becomes

$$\frac{da}{dt} = \frac{D}{\delta} \frac{\sigma T}{D_L(1 - K)mH} \left(\frac{1}{R} - \frac{1}{a} \right) \quad (9)$$

This kinetic equation implies a proportionality of a to $t^{1/2}$. In the absence of convection [18] the equation is similar to Equation 9, except that δ is replaced by a, hence a is proportional to $t^{1/3}$.

Following the same procedure as previously used for a system of n particles [17]

$$\frac{dr_i}{dt} = \sum_{\substack{j=1 \\ j \neq i}}^{n} \left[\frac{-D\sigma T}{C_L(1 - K)m_L H\delta} \left(\frac{1}{r_i} - \frac{1}{r_j} \right) \mathcal{H}(r_j - r_i) + \frac{-D\sigma T r_j}{C_L(1 - K)m_L H r_i \delta} \left(\frac{1}{r_i} - \frac{1}{r_j} \right) \mathcal{H}(r_i - r_j) \right] \quad (10)$$

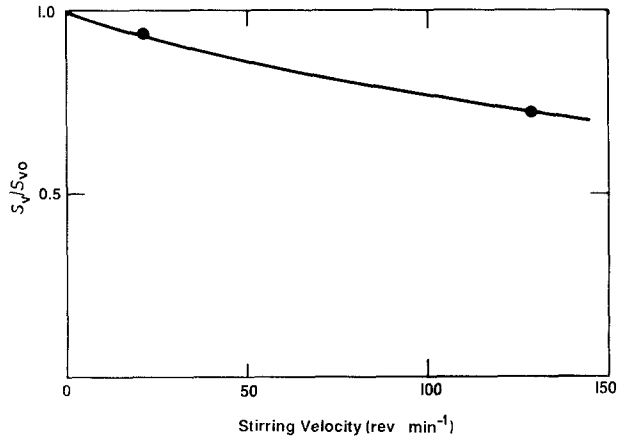

Figure 17 S_v/S_{vo} against stirring velocity for coarsening at 829 K ($f_s = 0.4$), for 10 h. Al–20 wt % Cu alloy, $S_{vo} = 9.4 \times 10^4 m^{-1}$.

The radius of the sphere i as a function of time is given by Equation 2. Hence, S_v can be calculated as a function of time.

This analysis was applied to Al–20 wt % Cu alloy at 829 K ($f_s = 0.4$), using the same initial population of 18 spheres and the same parameter values with various values of δ. A value of $\delta = 55 \mu m$ yielded a curve which is very close to the experimental curve of S_v/S_{vo} against isothermal coarsening time in the presence of forced convection, Fig. 15. The diffusion boundary layer thickness, δ, is a fraction of the average particle radius.

4. Conclusions

1. Isothermal dendritic or particulate coarsening is faster at higher temperatures and lower solute concentrations.

2. Turbulent fluid flow in the mushy zone may penetrate between primary, not secondary, dendrite arms. Its effect on coarsening is manifested only for longer holding times (500 sec).

3. At higher impeller angular velocities the dendritic structure breaks down into fragments which spheroidize rapidly.

4. Isothermal dendritic coarsening in the absence of convection operates in two stages: in stage I the dendritic structure breaks down through remelting into fragments which spheroidize quickly; in stage II the spherical particles coarsen slowly.

5. Alloy inoculation with titanium slows coarsening, yielding finer dendritic microstructures.

6. At lower shear rates of solid–liquid mixtures,

solid particles coalesce into clusters, whereas at higher rates (above about 650 rev. min^{-1}) the aggregates break up again into individual particles.

7. A coarsening model introduced here showed that coarsening is faster in the presence of forced convection, because of a consequent decrease in solute diffusion-boundary layer thickness.

Acknowledgement

The authors gratefully acknowledge the support of the University of Connecticut Research Foundation.

References

1. T. Z. KATTAMIS and J. C. LECOMTE, *J. Mater. Sci.* **13** (1978) 2731.
2. P. W. PETERSON, T. Z. KATTAMIS and A. F. GIAMEI, *Met. Trans. A* **11A** (1980) 1059.
3. S. D. RIDDLER, S. KOU and R. MEHRABIAN, *Met. Trans. B* **12B** (1981) 435.
4. M. J. STEWART and F. WEINBERG, *Met. Trans.* **3** (1972) 333.
5. K. SASKI, Y. SUGITANI, S. KOBEYASHI and S. ISHIMURA, *Tetsu-to Hagane* **65** (1979) 60.
6. T. MOMONO and K. IKAWA, *Trans. Jpn Inst. Metals* **19** (1978) 537.
7. J. P. GABATHULER and F. WEINBERG, *Met. Trans. B* **14B** (1983) 731.
8. N. STREAT and F. WEINBERG, *Met. Trans.* **3** (1972) 3181.
9. T. Z. KATTAMIS, Proceedings of the International Symposium on "Quality Control, of Engineering Alloys and the Role of Metals Science", Delft University of Technology, Delft, The Netherlands, March 1977, p. 189.
10. T. Z. KATTAMIS and J. C. LECOMTE, Proceedings of the 20th Colloque de Metallurgie on "Aspets Théoriques et Pratiques de la Solidification", Centre d'Etudes Nucléaires de Saclay, I.N.S.T.N., Gif-sur-Yvette, France, June 1977, p. 113.
11. T. Z. KATTAMIS, J. C. COUGHLIN and M. C. FLEMINGS, *Trans. TMS-AIME* **239** (1967) 1504.
12. D. B. SPENCER, R. MEHRABIAN and M. C. FLEMINGS, *Met. Trans.* **3** (1972) 1925.
13. E. E. UNDERWOOD, "Quantitative Stereology" (Addison-Wesley, Reading, 1970).
14. H. D. BRODY and M. C. FLEMINGS, *Trans. TMS-AIME* **236** (1966) 615.
15. V. G. LEVICH, "Physicochemical Hydrodynamics" (Prentice Hall, New York, 1962).
16. A. VOGEL, D Phil Thesis, University of Sussex (1977).
17. A. S. MICHAELS and J. C. BOLGER, *Ind. Eng. Chem. Fund.* **1** (3) (1962) 153.
18. N. J. WHISLER and T. Z. KATTAMIS, *J. Mater. Sci.* **7** (1972) 888.
19. *Idem, J. Cryst. Growth* **15** (1972) 20.

Received 24 August
and accepted 1 December 1987